JOURNAL OF MATERIALS PROCESSING TECHNOLOGY 208 (2008) 556–557

ELSEVIER

available at www.sciencedirect.com

ScienceDirect

journal homepage: www.elsevier.com/locate/jmatprotec

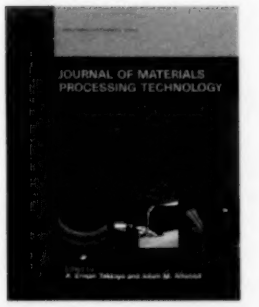

Author Index of Volume 208

Akbari Mousavi, S.A.A., 383
Aksogan, O., 299
Alagheband, A., 336
Amoruso, S., 409
Ausanio, G., 409

Bai, J., 251
Barone, A.C., 409
Bell, J.M., 117
Bin, H., 284
Binici, H., 299
Bocher, P., 542
Bochniak, W., 366
Bonny, K., 423
Buffa, G., 309
Butler, D.L., 14

Campana, C., 409
Camurri, C., 450
Camurri, C.P., 415
Cao, M., 145
Carrasco, C., 450
Chen, C.-C., 270
Chen, H., 9
Chen, J., 255
Chen, J.-H., 149
Chen, L., 90
Chen, T., 259, 395
Chen, Y.-L., 165
Chen, Z.H., 29
Cheng, J., 222
Cheng, Y.Q., 29
Cheung, F.Y., 196
Chiang, K.-T., 532
Choi, H., 211

Danno, A., 53
Date, P.P., 486
De Baets, P., 423
Demir, B., 75
Deng-long, W., 463
Derfuss, B., 444
Dille, J., 450
Ding, P., 342
Dong, Z., 1
Duan, H., 494
Dunnill, C.W., 520

El-Tayeb, N.S.M., 135
Erdoğan, M., 75

Fan, G.-W., 165
Fan, Y., 63
Feng, H.K., 330
Feng, K., 264
Feng, P.F., 124
Feng, Y., 222
Fratini, L., 309
Fredericks, P.M., 117

García-Navas, V., 187
García-Rosales, C., 187
Geddam, A., 196
Gheidari, A.M., 514
Gong, L.Y., 330
Gopukumar, S., 520
Gregory, D.H., 520
Gruhl, M., 444
Grzesik, W., 187
Gu, W.-C., 9
Guan, A., 342
Guo, Z., 457
Guoyi, T., 159
Gutman, E.M., 395

Hacini, L., 542
Hajidavalloo, E., 336
Hao, J., 457
Hao, Y., 395
He, J., 549
He, W., 205
He, Z., 90
Hedström, P., 415
Hengjun, L., 284
Hibbard, G.D., 507
Hira, S., 171
Hison, C., 409
Ho, S., 507
Hong, M., 264
Horng, J.-T., 532
Hsu, R.T., 318
Hu, L., 205
Huang, J.-H., 99
Huang, Y.-C., 24
Hui-chao, C., 463

Iannotti, V., 409

Ji, R.J., 245
Jiang, H., 229
Jing-lian, F., 463
Jung, I.D., 111
Jung, J.P., 179
Jung, P.G., 111
Junxi, W., 159

Kailas, S.V., 372
Kaplan, H., 299
Kavei, G., 514
Kermouche, G., 187
Kero, I., 415
Khellouki, A., 187
Kim, N., 211
Kishore, 372
Ko, J.S., 111
Kore, S.D., 486
Koren, Z., 395
Kulkarni, S.V., 486

Laizhu, J., 130
Lan, S., 264
Lanotte, L., 409
Lauwers, B., 423
Lee, G.-T., 42
Lee, S.M., 111
Lee, Y.-H., 35
Li, C.-H., 270
Li, D., 90
Li, F., 494
Li, H., 255
Li, J., 90, 105
Li, J.-Y., 165
Li, K.Y., 196
Li, L., 9
Li, M., 251
Li, Q.Y., 245
Li, X.P., 245, 400
Li, Y., 289, 457
Li, Y.L., 330
Liechty, B.C., 431
Liew, K.W., 135
Lin, C.-J., 149
Lin, X., 494
Liu, G., 494
Liu, H., 145
Liu, N.-M., 532
Liu, Q., 105
Liu, W., 423
Liu, X.-H., 42
Liu, Y.H., 245
Long, X., 229
Lum, I., 179
Luo, D., 145
Lv, G.-H., 9

Maeda, Y., 400
Mangalaraja, R.V., 415
Mayer, M., 179
Mazurkiewicz, D., 477

Elsevier B.V.
doi:10.1016/S0924-0136(08)00692-4

Meini, Y., 284
Menezes, P.L., 372
Meng, G., 229
Miresmaeili, R., 383
Mizuno, M., 159
Mouzon, J., 415

Nakahara, T., 507
Neo, K.S., 400
Nguyen, A.T., 14
Ning, L., 130
Niu, E.-W., 9

Odén, M., 415
Ozerdem, M.S., 470

Pantoł, K., 366
Park, H.-D., 42
Paulmier, T., 117
Piacentini, M., 309
Pramanik, A., 400

Qian, Y.-P., 99
Qiang, Y., 159
Qin, L., 255
Qu, B., 342

Rahman, M., 400
Ramam, K.V.S., 415
Rech, J., 187
Ren, S., 457
Rosenson, H., 395
Rottmair, C.A., 444

Salehi, A., 423
Sawa, M., 400
Shah, T., 299
Shi, R.-x., 105
Shi, Z., 259
Shih, H.-H., 24
Singer, R.F., 444
Sivashanmugam, A., 520
Sugiyama, S., 165
Sun, H., 205
Sun, L.W., 318

Tamaki, J., 239
Tan, J., 222
Tang, Q., 90
Tang, X., 549
Tao, L., 463
Thirunakaran, R., 520
Tian, Y., 179
Tong, H., 289
Tong, K.K., 53
Tsai, F.C., 318
Tsai, M.-J., 149, 270
Tsai, Y.-L., 35

Uhlmann, E., 124
Unigovski, Y., 395

Van der Biest, O., 423
Van Lê, N., 542
Vleugels, J., 423
Volek, A., 444

Wang, C., 179
Wang, E., 205
Wang, G.-L., 99
Wang, S.-Y., 149
Wang, Y., 289
Webb, B.W., 431
Wei, L., 499
Wei, W., 222
Wei, Y., 1
Wei, Z., 130
Wen, Y., 105
Wong, C.C., 53
Wu, J., 264
Wu, Y.-S., 35
Wu, Z.J., 124

Xian, K.F., 29
Xian, L., 284
Xiaodong, W., 63
Xie, J., 239
Xu, G., 549
Xu, L., 494
Xu, P., 549
Xue, C., 255

Yan, B.H., 318
Yanagimoto, J., 165
Yang, Q., 251
Yang, S.-Z., 9
Yang, T.-H., 149
Yang, Y., 264
Yang, Z., 255
Yanqing, Y., 284
Yao, S., 549
Yi, L., 63
Yiaoxian, L., 251
Yin, Y.-s., 105
Yingchun, G., 159
Yong, M.S., 53
Yongbo, W., 159
Yoshioka, M., 171
Yu, D.W., 124
Yu, H., 145
Yu, H.-L., 42
Yu, L.L., 245
Yu, S.R., 330
Yu, Y., 205
Yuhua, W., 130
Yuying, Y., 499

Zhan, X., 1
Zhang, B., 171
Zhang, C., 251
Zhang, H., 29
Zhang, H.F., 245
Zhang, H.-O., 99
Zhang, J., 70
Zhang, M., 342
Zhang, X.-H., 9
Zhang, Y., 70, 85
Zhang, Z., 85
Zhao, S., 85
Zhou, H., 90
Zhou, Y., 179
Zhou, Z.F., 196
Zhuang, H., 255

JOURNAL OF MATERIALS PROCESSING TECHNOLOGY 208 (2008) 558–566

available at www.sciencedirect.com

ScienceDirect

journal homepage: www.elsevier.com/locate/jmatprotec

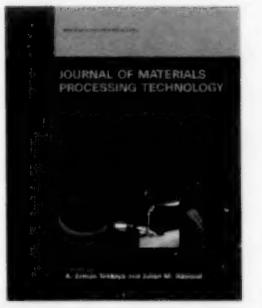

Subject Index of Volume 208

Abrasive jet polishing
Abrasive jet polishing on SKD61 mold steel using SiC coated with Wax, 318
Accuracy
Direct rapid high-temperature alloy prototyping by hybrid plasma-laser technology, 99
Adjoining Vickers indentations
Experimental observation and numerical analysis of cracking phenomena in adjoining Vickers indentations on glass surface, 171
Alloy content
The hardenability of austenite with different alloy content and dispersion in dual-phase steels, 75
Al-to-SS welding
Electromagnetic impact welding of aluminum to stainless steel sheets, 486
Ammonium perchlorate
Synthesis of Ni nanoparticles and their catalytic effect on the decomposition of ammonium perchlorate, 494
Ammonium polyphosphate
A new method to prepare flame retardant polymer composites, 342
Anodic oxidation
Study on the black electrolytic coloring of anodized aluminum in cupric sulfate, 24
Anodizing
Effect of processing on stress-corrosion behavior of die-cast Mg–Al alloy, 395
Array electrode
Experimental research on vibration assisted EDM of micro-structures with non-circular cross-section, 289
Artificial neural network (ANN)
Optimal laser-cutting parameters for QFN packages by utilizing artificial neural networks and genetic algorithm, 270
Artificial neural network approach to predict the electrical conductivity and density of Ag–Ni binary alloys, 470
Atomic force microscopy (AFM)
The effects of surface roughness and nanostructure on the properties of indium tin oxide (ITO) designated for novel optoelectronic devices fabrication, 514
AZ31 magnesium alloy sheet
Flow stress equation of AZ31 magnesium alloy sheet during warm tensile deformation, 29

Back transfer films
Effect of water spray on friction and wear behaviour of noncommercial and commercial brake pad materials, 135
Belt conveyor
Analysis of the ageing impact on the strength of the adhesive sealed joints of conveyor belts, 477
Belt finishing
Characterization and modelling of the residual stresses induced by belt finishing on a AISI52100 hardened steel, 187
Black electrolytic coloring
Study on the black electrolytic coloring of anodized aluminum in cupric sulfate, 24
Bonded joint
Analysis of the ageing impact on the strength of the adhesive sealed joints of conveyor belts, 477

$CaCu_3Ti_4O_{12}$
Microwave synthesis of high dielectric constant $CaCu_3Ti_4O_{12}$, 145
β-Cyclodextrin
Synthesis of poly(*N*-vinylpyrrolidone)/β-cyclodextrin composite nanofibers using electrospinning techniques, 251
Carbon mesophase
Net-shape production of graphite parts via powder injection moulding of carbon mesophase, 444
Catalytic effect
Synthesis of Ni nanoparticles and their catalytic effect on the decomposition of ammonium perchlorate, 494
Cellular automaton
Cellular automaton simulation of grain growth with different orientation angles during solidification process, 1
Cellulose ether
Gelcasting of metal powders in nontoxic cellulose ethers system, 457
Ceramic tool
Investigating the machinability evaluation of Hadfield steel in the hard turning with Al_2O_3/TiC mixed ceramic tool based on the response surface methodology, 532
Chemical machining
Chemical machining of nanocrystalline Ni, 507
Coating
Plasma electrolytic deposition of titanium dioxide nanorods and nano-particles, 117
Cobaltite ceramics
Rapid reactive synthesis and sintering of textured $Ca_3Co_4O_9$ ceramics by spark plasma sintering, 70
Combustion
Combustion synthesis of Y_2O_3 and Yb–Y_2O_3. Part I. Nanopowders and their characterization, 415

Elsevier B.V.
doi:10.1016/S0924-0136(08)00693-6

Composites
The improvement on capacity retention of silicon/graphite composites with TiN additive as anode materials for Li-ion battery, 35
Preparation and mechanical properties of Fe_3Al(Ti)/TiC composites, 105
Computation model
An improved computation model for critical bending force of three-jaw chucks, 124
Concrete
Durability of concrete made with granite and marble as recycle aggregates, 299
COP (cyclo-olefin polymer) microfluidic chip
Microfluidic chip made of COP (cyclo-olefin polymer) and comparion to PMMA (polymethylmethacrylate) microfluidic chip, 63
Copper sulfate
Study on the black electrolytic coloring of anodized aluminum in cupric sulfate, 24
Copper wire
Investigation of ultrasonic copper wire wedge bonding on Au/Ni plated Cu substrates at ambient temperature, 179
Coprecipitation method
Rapid reactive synthesis and sintering of textured $Ca_3Co_4O_9$ ceramics by spark plasma sintering, 70
Corrosion
Chemical machining of nanocrystalline Ni, 507
Corrosion creep
Effect of processing on stress-corrosion behavior of die-cast Mg–Al alloy, 395
Corrosion resistance
Effects of current frequency on the structural characteristics and corrosion property of ceramic coatings formed on magnesium alloy by PEO technology, 9
Corrosive solutions
Effect of processing on stress-corrosion behavior of die-cast Mg–Al alloy, 395
Critical bending force
An improved computation model for critical bending force of three-jaw chucks, 124
Crystallographic axes orientation
Cellular automaton simulation of grain growth with different orientation angles during solidification process, 1
Cu–Cr alloy
Effect of extrusion on microstructure and properties of a submicron crystalline Cu–5 wt.%Cr alloy, 205
Current frequency
Effects of current frequency on the structural characteristics and corrosion property of ceramic coatings formed on magnesium alloy by PEO technology, 9
Cutting edge radius
Cutting edge preparation using magnetic polishing and its influence on the performance of high-speed steel drills, 196
Cutting vibration
Study of the correlation between surface generation and cutting vibrations in peripheral milling, 229
Cyclicform rolling
Structure of copper subjected to changes of the loading scheme during rolling, 366
Decomposition
Synthesis of Ni nanoparticles and their catalytic effect on the decomposition of ammonium perchlorate, 494
Densification
Numerical simulation of the densification processing of titanium-matrix coated fiber composites, 284
Density
Artificial neural network approach to predict the electrical conductivity and density of Ag–Ni binary alloys, 470
Design of experiment (DOE)
Investigation of ultrasonic copper wire wedge bonding on Au/Ni plated Cu substrates at ambient temperature, 179
Diamond grinding wheel
An experimental study on discharge mediums used for electro-contact discharge dressing of metal-bonded diamond grinding wheel, 239
Diamond tool
Ultra-precision turning of electroless-nickel: Effect of phosphorus contents, depth-of-cut and rake angle, 400
Dielectrics
Microwave synthesis of high dielectric constant $CaCu_3Ti_4O_{12}$, 145
Die-sinking EDM
Experimental research on vibration assisted EDM of micro-structures with non-circular cross-section, 289
Direct rapid high-temperature alloy prototyping
Direct rapid high-temperature alloy prototyping by hybrid plasma-laser technology, 99
Discharge medium
An experimental study on discharge mediums used for electro-contact discharge dressing of metal-bonded diamond grinding wheel, 239
Distortion
Experimental and numerical analyses of residual stress distributions in TIG welding process for 304L stainless steel, 383
DNA separation
Microfluidic chip made of COP (cyclo-olefin polymer) and comparion to PMMA (polymethylmethacrylate) microfluidic chip, 63
Drilling
Cutting edge preparation using magnetic polishing and its influence on the performance of high-speed steel drills, 196
Dry sliding
Influence of secondary electro-conductive phases on the electrical discharge machinability and frictional behavior of ZrO_2-based ceramic composites, 423
Dual-phase steels
The hardenability of austenite with different alloy content and dispersion in dual-phase steels, 75
Durability
Durability of concrete made with granite and marble as recycle aggregates, 299
Dynamic modulus of elasticity
Grading of softwood lumber using non-destructive techniques, 149
Dynamic recovery
Effect of extrusion on microstructure and properties of a submicron crystalline Cu–5 wt.%Cr alloy, 205
The prediction of deformation behavior and interfacial friction under hot working conditions using inverse analysis, 211

Dynamic recrystallization
Effect of extrusion on microstructure and properties of a submicron crystalline Cu–5 wt.%Cr alloy, 205
The prediction of deformation behavior and interfacial friction under hot working conditions using inverse analysis, 211
Dynamical observation of indentation process
Experimental observation and numerical analysis of cracking phenomena in adjoining Vickers indentations on glass surface, 171

ECA pressing
Improvement of shape memory effect in an Fe–Mn–Si–Cr–Ni alloy fabricated by equal channel angular pressing, 130
Electric discharge machining
Effect of technological parameter on the process performance for electric discharge milling of insulating Al_2O_3 ceramic, 245
Electric discharge milling
Effect of technological parameter on the process performance for electric discharge milling of insulating Al_2O_3 ceramic, 245
Electric energy saving
Thermal analysis of sponge iron preheating using waste energy of EAF, 336
Electric field
Intensified sintering of iron powders under the action of an electric field: Effect of technologic parameter on sintering densification, 264
Electrical conductivity
Artificial neural network approach to predict the electrical conductivity and density of Ag–Ni binary alloys, 470
Electro-contact discharge dressing
An experimental study on discharge mediums used for electro-contact discharge dressing of metal-bonded diamond grinding wheel, 239
Electrodeposition
Chemical machining of nanocrystalline Ni, 507
Electroless-nickel
Ultra-precision turning of electroless-nickel: Effect of phosphorus contents, depth-of-cut and rake angle, 400
Electromagnetic
Electromagnetic impact welding of aluminum to stainless steel sheets, 486
Electron microscopy
Synthesis of poly(*N*-vinylpyrrolidone)/β-cyclodextrin composite nanofibers using electrospinning techniques, 251
Electrospinning
Synthesis of poly(*N*-vinylpyrrolidone)/β-cyclodextrin composite nanofibers using electrospinning techniques, 251
Extrusion
Effect of extrusion on microstructure and properties of a submicron crystalline Cu–5 wt.%Cr alloy, 205

Fe_3Al
Preparation and mechanical properties of $Fe_3Al(Ti)/TiC$ composites, 105
Fine grains
Structure of copper subjected to changes of the loading scheme during rolling, 366
Fine-grained tungsten heavy alloy
Preparation of fine grain tungsten heavy alloy with high properties by mechanical alloying and yttrium oxide addition, 463
Finite element analysis
Multi-objective optimization of sheet metal forming process using Pareto-based genetic algorithm, 499
Finite element (FE) simulation
A novel response variable for finite element simulation of hydro-mechanical deep drawing, 85
Finite element method
Experimental and numerical analyses of residual stress distributions in TIG welding process for 304L stainless steel, 383
Finite element model
Characterization and modelling of the residual stresses induced by belt finishing on a AISI52100 hardened steel, 187
Numerical simulation of the densification processing of titanium-matrix coated fiber composites, 284
Finite Element simulation
Cold rotary forming of thin-wall component from flat-disc blank, 53
Fixed bed
Thermal analysis of sponge iron preheating using waste energy of EAF, 336
Flow forming
Cold rotary forming of thin-wall component from flat-disc blank, 53
Flow stress
Flow stress equation of AZ31 magnesium alloy sheet during warm tensile deformation, 29
Flow stress function
The prediction of deformation behavior and interfacial friction under hot working conditions using inverse analysis, 211
Flue gas
Thermal analysis of sponge iron preheating using waste energy of EAF, 336
Forming limit diagram (FLD)
A novel response variable for finite element simulation of hydro-mechanical deep drawing, 85
Friction
Effect of water spray on friction and wear behaviour of noncommercial and commercial brake pad materials, 135
Effect of surface roughness parameters and surface texture on friction and transfer layer formation in tin–steel tribo-system, 372
Friction coefficient
Influence of secondary electro-conductive phases on the electrical discharge machinability and frictional behavior of ZrO_2-based ceramic composites, 423
Friction stir processing
Flow field characterization of friction stir processing using a particle-grid method, 431
Frictional brake pad
Effect of water spray on friction and wear behaviour of noncommercial and commercial brake pad materials, 135
Fuzzy evaluation
Optimization of injection mold based on fuzzy moldability evaluation, 222

GAIM
A study on gas-assisted injection molding filling simulation based on surface model of a contained circle channel part, 90
GaN
Structure and luminescent properties of GaN nanorods grown by magnetron sputtering and ammoniating technique, 255

Gas atomization
Abrasive jet polishing on SKD61 mold steel using SiC coated with Wax, 318
Gas channel
A study on gas-assisted injection molding filling simulation based on surface model of a contained circle channel part, 90
Gas penetration
A study on gas-assisted injection molding filling simulation based on surface model of a contained circle channel part, 90
Gelcasting
Gelcasting of metal powders in nontoxic cellulose ethers system, 457
Generation of microcracks
Experimental observation and numerical analysis of cracking phenomena in adjoining Vickers indentations on glass surface, 171
Genetic algorithm (GA)
Optimal laser-cutting parameters for QFN packages by utilizing artificial neural networks and genetic algorithm, 270
Glass surface
Experimental observation and numerical analysis of cracking phenomena in adjoining Vickers indentations on glass surface, 171
GMR effect
Evidence of giant magnetoresistance effect in heterogeneous nanogranular films produced by ultrashort pulsed laser deposition, 409
Gouging
A tool path generation strategy for three-axis ball-end milling of free-form surfaces, 259
Grain growth
Cellular automaton simulation of grain growth with different orientation angles during solidification process, 1
Grain refining
Improvement of shape memory effect in an Fe–Mn–Si–Cr–Ni alloy fabricated by equal channel angular pressing, 130
Granite
Durability of concrete made with granite and marble as recycle aggregates, 299
Grinding
Correlation of grinding wheel topography and grinding performance: A study from a viewpoint of three-dimensional surface characterisation, 14
Grinding balls
Residual stress during heat treatment of steel grinding balls, 450
Groove
Experimental and numerical analyses of residual stress distributions in TIG welding process for 304L stainless steel, 383
Ground blast furnace slag
Durability of concrete made with granite and marble as recycle aggregates, 299

Hadfield steel
Investigating the machinability evaluation of Hadfield steel in the hard turning with Al_2O_3/TiC mixed ceramic tool based on the response surface methodology, 532
Hammer peening
Effect of impact energy on residual stresses induced by hammer peening of 304L plates, 542
Hard turning
Characterization and modelling of the residual stresses induced by belt finishing on a AISI52100 hardened steel, 187
Investigating the machinability evaluation of Hadfield steel in the hard turning with Al_2O_3/TiC mixed ceramic tool based on the response surface methodology, 532
Hardenability
The hardenability of austenite with different alloy content and dispersion in dual-phase steels, 75
Heat treatment
Residual stress during heat treatment of steel grinding balls, 450
High-frequency vibration
Experimental research on vibration assisted EDM of micro-structures with non-circular cross-section, 289
Hot embossing
Microfluidic chip made of COP (cyclo-olefin polymer) and comparion to PMMA (polymethylmethacrylate) microfluidic chip, 63
Hydrogen plasma method
Synthesis of Ni nanoparticles and their catalytic effect on the decomposition of ammonium perchlorate, 494
Hydro-mechanical deep drawing
A novel response variable for finite element simulation of hydro-mechanical deep drawing, 85
Hypereutectic Al–Si alloy
Effect of ultrasonic treatment on microstructures of hypereutectic Al–Si alloy, 330

Impact
Electromagnetic impact welding of aluminum to stainless steel sheets, 486
Impact energy
Effect of impact energy on residual stresses induced by hammer peening of 304L plates, 542
Incremental forming
Cold rotary forming of thin-wall component from flat-disc blank, 53
Injection mold
Optimization of injection mold based on fuzzy moldability evaluation, 222
Insulating ceramics
Effect of technological parameter on the process performance for electric discharge milling of insulating Al_2O_3 ceramic, 245
Interfacial friction
The prediction of deformation behavior and interfacial friction under hot working conditions using inverse analysis, 211
Inverse analysis
The prediction of deformation behavior and interfacial friction under hot working conditions using inverse analysis, 211
Inverse peritectic
Effect of inverse peritectic reaction on microstructural spheroidization in semi-solid state, 165
Iron powders
Intensified sintering of iron powders under the action of an electric field: Effect of technologic parameter on sintering densification, 264
Isotropic hardening
Experimental and numerical analyses of residual stress distributions in TIG welding process for 304L stainless steel, 383

Kinematic hardening
Experimental and numerical analyses of residual stress distributions in TIG welding process for 304L stainless steel, 383

Laser clad
Effect of Y_2O_3 addition on microstructure of Ni-based alloy + Y_2O_3/substrate laser clad, 549
Laser cutting
Optimal laser-cutting parameters for QFN packages by utilizing artificial neural networks and genetic algorithm, 270
Latin hypercube design
Multi-objective optimization of sheet metal forming process using Pareto-based genetic algorithm, 499
Layered double hydroxide
A new method to prepare flame retardant polymer composites, 342
Levenberg–Marquardt (LM) algorithm
Optimal laser-cutting parameters for QFN packages by utilizing artificial neural networks and genetic algorithm, 270
$Li_{2.6}Co_{0.4}N$
Studies on chromium/aluminium-doped manganese spinel as cathode materials for lithium-ion batteries—A novel chelated sol–gel synthesis, 520
$LiAl_xMn_{2-x}O_4$
Studies on chromium/aluminium-doped manganese spinel as cathode materials for lithium-ion batteries—A novel chelated sol–gel synthesis, 520
$LiCr_xMn_{2-x}O_4$
Studies on chromium/aluminium-doped manganese spinel as cathode materials for lithium-ion batteries—A novel chelated sol–gel synthesis, 520
Li-ion battery
The improvement on capacity retention of silicon/graphite composites with TiN additive as anode materials for Li-ion battery, 35
$LiMn_2O_4$
Studies on chromium/aluminium-doped manganese spinel as cathode materials for lithium-ion batteries—A novel chelated sol–gel synthesis, 520
Lithium-ion battery
Studies on chromium/aluminium-doped manganese spinel as cathode materials for lithium-ion batteries—A novel chelated sol–gel synthesis, 520
Long cutting distance
Ultra-precision turning of electroless-nickel: Effect of phosphorus contents, depth-of-cut and rake angle, 400
Long-term strength
Analysis of the ageing impact on the strength of the adhesive sealed joints of conveyor belts, 477
Luminescence
Structure and luminescent properties of GaN nanorods grown by magnetron sputtering and ammoniating technique, 255
L-Value
Study on the black electrolytic coloring of anodized aluminum in cupric sulfate, 24

MA
Preparation of fine grain tungsten heavy alloy with high properties by mechanical alloying and yttrium oxide addition, 463
Machinability
Investigating the machinability evaluation of Hadfield steel in the hard turning with Al_2O_3/TiC mixed ceramic tool based on the response surface methodology, 532
Machine stress grading
Grading of softwood lumber using non-destructive techniques, 149
Magnesium
Effects of current frequency on the structural characteristics and corrosion property of ceramic coatings formed on magnesium alloy by PEO technology, 9
Magnetic polishing
Cutting edge preparation using magnetic polishing and its influence on the performance of high-speed steel drills, 196
Magnetoresistance
Evidence of giant magnetoresistance effect in heterogeneous nanogranular films produced by ultrashort pulsed laser deposition, 409
Marble
Durability of concrete made with granite and marble as recycle aggregates, 299
Martensite
Improvement of shape memory effect in an Fe–Mn–Si–Cr–Ni alloy fabricated by equal channel angular pressing, 130
Residual stress during heat treatment of steel grinding balls, 450
Material flow
Flow field characterization of friction stir processing using a particle-grid method, 431
Material removal rate
Influence of secondary electro-conductive phases on the electrical discharge machinability and frictional behavior of ZrO_2-based ceramic composites, 423
MCMB
Net-shape production of graphite parts via powder injection moulding of carbon mesophase, 444
Mechanical properties
Preparation and mechanical properties of Fe_3Al(Ti)/TiC composites, 105
A new method to prepare flame retardant polymer composites, 342
Metal powder
Gelcasting of metal powders in nontoxic cellulose ethers system, 457
Microchannel
Fabrication of self-encapsulated nickel microchannels and nickel nanowalls by reactive ion etching, 111
Micro-EDM
Experimental research on vibration assisted EDM of micro-structures with non-circular cross-section, 289
Microstructure
Effect of inverse peritectic reaction on microstructural spheroidization in semi-solid state, 165
On the influence of tool path in friction stir spot welding of aluminum alloys, 309
Effect of ultrasonic treatment on microstructures of hypereutectic Al–Si alloy, 330
Microwave synthesis
Microwave synthesis of high dielectric constant $CaCu_3Ti_4O_{12}$, 145
Mirror machining
Abrasive jet polishing on SKD61 mold steel using SiC coated with Wax, 318

Moldability
Optimization of injection mold based on fuzzy moldability evaluation, 222
Multi-objective genetic algorithm
Multi-objective optimization of sheet metal forming process using Pareto-based genetic algorithm, 499
Multiphase nitride inclusions
The effect of multiphase nitride inclusions on the surface roughness of 2083 plastic molds, 159
Multiple regression analysis (MRA)
Optimal laser-cutting parameters for QFN packages by utilizing artificial neural networks and genetic algorithm, 270

Nanocrystalline
Chemical machining of nanocrystalline Ni, 507
Nanocrystalline powders
Combustion synthesis of Y_2O_3 and Yb–Y_2O_3. Part I. Nanopowders and their characterization, 415
Nanofibers
Synthesis of poly(*N*-vinylpyrrolidone)/β-cyclodextrin composite nanofibers using electrospinning techniques, 251
Nanogranular magnetic films
Evidence of giant magnetoresistance effect in heterogeneous nanogranular films produced by ultrashort pulsed laser deposition, 409
Nanorods
Structure and luminescent properties of GaN nanorods grown by magnetron sputtering and ammoniating technique, 255
Nanostructure
Plasma electrolytic deposition of titanium dioxide nanorods and nano-particles, 117
Nanowall
Fabrication of self-encapsulated nickel microchannels and nickel nanowalls by reactive ion etching, 111
NC machining
A tool path generation strategy for three-axis ball-end milling of free-form surfaces, 259
Ni nanoparticles
Synthesis of Ni nanoparticles and their catalytic effect on the decomposition of ammonium perchlorate, 494
Ni-based alloy + Y_2O_3
Effect of Y_2O_3 addition on microstructure of Ni-based alloy + Y_2O_3/substrate laser clad, 549
Nickel
Fabrication of self-encapsulated nickel microchannels and nickel nanowalls by reactive ion etching, 111
Chemical machining of nanocrystalline Ni, 507
Non-circular cross-section electrode
Experimental research on vibration assisted EDM of micro-structures with non-circular cross-section, 289
Non-destructive technique
Grading of softwood lumber using non-destructive techniques, 149
Numerical method
Numerical analysis of strip edge drop for Sendzimir mill, 42
Numerical simulation
A study on gas-assisted injection molding filling simulation based on surface model of a contained circle channel part, 90

Optical property
A new method to prepare flame retardant polymer composites, 342
Pentaerythritol
A new method to prepare flame retardant polymer composites, 342
Peripheral milling
Study of the correlation between surface generation and cutting vibrations in peripheral milling, 229
Perovskite
Microwave synthesis of high dielectric constant $CaCu_3Ti_4O_{12}$, 145
Phase transformation
The hardenability of austenite with different alloy content and dispersion in dual-phase steels, 75
Phenolic resin
The improvement on capacity retention of silicon/graphite composites with TiN additive as anode materials for Li-ion battery, 35
PIM
Net-shape production of graphite parts via powder injection moulding of carbon mesophase, 444
Plasma electrolytic deposition
Plasma electrolytic deposition of titanium dioxide nanorods and nano-particles, 117
Plasma electrolytic oxidation
Effects of current frequency on the structural characteristics and corrosion property of ceramic coatings formed on magnesium alloy by PEO technology, 9
Plasma-laser deposition manufacturing (PLDM)
Direct rapid high-temperature alloy prototyping by hybrid plasma-laser technology, 99
Plastic mold steel
The effect of multiphase nitride inclusions on the surface roughness of 2083 plastic molds, 159
Polishing
The effect of multiphase nitride inclusions on the surface roughness of 2083 plastic molds, 159
Preheating
Thermal analysis of sponge iron preheating using waste energy of EAF, 336

Q quality factor
The effects of surface roughness and nanostructure on the properties of indium tin oxide (ITO) designated for novel optoelectronic devices fabrication, 514
QFN package
Optimal laser-cutting parameters for QFN packages by utilizing artificial neural networks and genetic algorithm, 270

Rare earth oxide dispersion
Preparation of fine grain tungsten heavy alloy with high properties by mechanical alloying and yttrium oxide addition, 463
Reactive ion etching
Fabrication of self-encapsulated nickel microchannels and nickel nanowalls by reactive ion etching, 111
Recrystallization
Investigation of ultrasonic copper wire wedge bonding on Au/Ni plated Cu substrates at ambient temperature, 179
Recycle aggregates
Durability of concrete made with granite and marble as recycle aggregates, 299
Refractory and intractable materials
Direct rapid high-temperature alloy prototyping by hybrid plasma-laser technology, 99

Residual stress
Experimental and numerical analyses of residual stress distributions in TIG welding process for 304L stainless steel, 383
Residual stress during heat treatment of steel grinding balls, 450
Residual stress relaxation
Effect of impact energy on residual stresses induced by hammer peening of 304L plates, 542
Residual stresses
Characterization and modelling of the residual stresses induced by belt finishing on a AISI52100 hardened steel, 187
Residual stresses measurement
Effect of impact energy on residual stresses induced by hammer peening of 304L plates, 542
Response surface methodology (RSM)
Investigating the machinability evaluation of Hadfield steel in the hard turning with Al_2O_3/TiC mixed ceramic tool based on the response surface methodology, 532
Response surface model
Multi-objective optimization of sheet metal forming process using Pareto-based genetic algorithm, 499
Response variable
A novel response variable for finite element simulation of hydro-mechanical deep drawing, 85
Rheoformed Mg alloy
Effect of processing on stress-corrosion behavior of die-cast Mg–Al alloy, 395
Rotary forming
Cold rotary forming of thin-wall component from flat-disc blank, 53
Roughness parameters
Effect of surface roughness parameters and surface texture on friction and transfer layer formation in tin–steel tribo-system, 372

Scanning probe microscopy (SPM)
The effects of surface roughness and nanostructure on the properties of indium tin oxide (ITO) designated for novel optoelectronic devices fabrication, 514
Semi-solid
Effect of inverse peritectic reaction on microstructural spheroidization in semi-solid state, 165
Sendzimir mill
Numerical analysis of strip edge drop for Sendzimir mill, 42
Shape memory alloy
Improvement of shape memory effect in an Fe–Mn–Si–Cr–Ni alloy fabricated by equal channel angular pressing, 130
Shear banding
Structure of copper subjected to changes of the loading scheme during rolling, 366
Sheet metal forming
A novel response variable for finite element simulation of hydro-mechanical deep drawing, 85
Multi-objective optimization of sheet metal forming process using Pareto-based genetic algorithm, 499
SiC fiber
Numerical simulation of the densification processing of titanium-matrix coated fiber composites, 284
Silicon
The improvement on capacity retention of silicon/graphite composites with TiN additive as anode materials for Li-ion battery, 35
Silver–nickel binary alloys
Artificial neural network approach to predict the electrical conductivity and density of Ag–Ni binary alloys, 470
Single crystal
Structure and luminescent properties of GaN nanorods grown by magnetron sputtering and ammoniating technique, 255
Sintering
Intensified sintering of iron powders under the action of an electric field: Effect of technologic parameter on sintering densification, 264
Preparation of fine grain tungsten heavy alloy with high properties by mechanical alloying and yttrium oxide addition, 463
Sol–gel method
Studies on chromium/aluminium-doped manganese spinel as cathode materials for lithium-ion batteries—A novel chelated sol–gel synthesis, 520
Solidification
Cellular automaton simulation of grain growth with different orientation angles during solidification process, 1
Spark plasma sintering
Rapid reactive synthesis and sintering of textured $Ca_3Co_4O_9$ ceramics by spark plasma sintering, 70
Spheroidization
Effect of inverse peritectic reaction on microstructural spheroidization in semi-solid state, 165
Sponge iron
Thermal analysis of sponge iron preheating using waste energy of EAF, 336
Spot
On the influence of tool path in friction stir spot welding of aluminum alloys, 309
Stainless steel
Experimental and numerical analyses of residual stress distributions in TIG welding process for 304L stainless steel, 383
Strain
Flow field characterization of friction stir processing using a particle-grid method, 431
Strain-rates
Flow field characterization of friction stir processing using a particle-grid method, 431
Stress field analysis
Experimental observation and numerical analysis of cracking phenomena in adjoining Vickers indentations on glass surface, 171
Stress field interference
Experimental observation and numerical analysis of cracking phenomena in adjoining Vickers indentations on glass surface, 171
Strip edge drop
Numerical analysis of strip edge drop for Sendzimir mill, 42
Structure refinement
Structure of copper subjected to changes of the loading scheme during rolling, 366
Submicron crystalline
Effect of extrusion on microstructure and properties of a submicron crystalline Cu–5 wt.%Cr alloy, 205
Superfinishing
Characterization and modelling of the residual stresses induced by belt finishing on a AISI52100 hardened steel, 187

Surface characterisation
Correlation of grinding wheel topography and grinding performance: A study from a viewpoint of three-dimensional surface characterisation, 14
Surface generation
Study of the correlation between surface generation and cutting vibrations in peripheral milling, 229
Surface integrity
Influence of secondary electro-conductive phases on the electrical discharge machinability and frictional behavior of ZrO_2-based ceramic composites, 423
Surface model
A study on gas-assisted injection molding filling simulation based on surface model of a contained circle channel part, 90
Surface roughness
The effect of multiphase nitride inclusions on the surface roughness of 2083 plastic molds, 159
An experimental study on discharge mediums used for electro-contact discharge dressing of metal-bonded diamond grinding wheel, 239
The effects of surface roughness and nanostructure on the properties of indium tin oxide (ITO) designated for novel optoelectronic devices fabrication, 514
Surface state
Direct rapid high-temperature alloy prototyping by hybrid plasma-laser technology, 99
Surface texture
Effect of surface roughness parameters and surface texture on friction and transfer layer formation in tin–steel tribo-system, 372
Suspension
Gelcasting of metal powders in nontoxic cellulose ethers system, 457
Synthesis
Combustion synthesis of Y_2O_3 and Yb–Y_2O_3. Part I. Nanopowders and their characterization, 415

Technologic parameter
Intensified sintering of iron powders under the action of an electric field: Effect of technologic parameter on sintering densification, 264
Technological parameter
Effect of technological parameter on the process performance for electric discharge milling of insulating Al_2O_3 ceramic, 245
Tensile strength
Electromagnetic impact welding of aluminum to stainless steel sheets, 486
Thermolelectric properties
Rapid reactive synthesis and sintering of textured $Ca_3Co_4O_9$ ceramics by spark plasma sintering, 70
Three-jaw chuck
An improved computation model for critical bending force of three-jaw chucks, 124
TiC
Preparation and mechanical properties of Fe_3Al(Ti)/TiC composites, 105
TIG
Experimental and numerical analyses of residual stress distributions in TIG welding process for 304L stainless steel, 383
TiN
The improvement on capacity retention of silicon/graphite composites with TiN additive as anode materials for Li-ion battery, 35
Titanium dioxide
Plasma electrolytic deposition of titanium dioxide nanorods and nano-particles, 117
Titanium matrix composites
Numerical simulation of the densification processing of titanium-matrix coated fiber composites, 284
Tool life
Cutting edge preparation using magnetic polishing and its influence on the performance of high-speed steel drills, 196
Tool path generation
A tool path generation strategy for three-axis ball-end milling of free-form surfaces, 259
Torch-heating
Effect of impact energy on residual stresses induced by hammer peening of 304L plates, 542
Transfer layer
Effect of surface roughness parameters and surface texture on friction and transfer layer formation in tin–steel tribo-system, 372
Triangulation
A tool path generation strategy for three-axis ball-end milling of free-form surfaces, 259
Truing ratio
An experimental study on discharge mediums used for electro-contact discharge dressing of metal-bonded diamond grinding wheel, 239

Ultra-precision machining
Ultra-precision turning of electroless-nickel: Effect of phosphorus contents, depth-of-cut and rake angle, 400
Ultrashort pulsed laser deposition
Evidence of giant magnetoresistance effect in heterogeneous nanogranular films produced by ultrashort pulsed laser deposition, 409
Ultrasonic softening
Investigation of ultrasonic copper wire wedge bonding on Au/Ni plated Cu substrates at ambient temperature, 179
Ultrasonic treatment
Effect of ultrasonic treatment on microstructures of hypereutectic Al–Si alloy, 330
Ultrasonic wedge bonding
Investigation of ultrasonic copper wire wedge bonding on Au/Ni plated Cu substrates at ambient temperature, 179
Unitary impact
Effect of impact energy on residual stresses induced by hammer peening of 304L plates, 542

Variable temperature quasi-creep experiment
Microfluidic chip made of COP (cyclo-olefin polymer) and comparion to PMMA (polymethylmethacrylate) microfluidic chip, 63
Variable weight profit vector
Optimization of injection mold based on fuzzy moldability evaluation, 222
Visible light reflectivity
Study on the black electrolytic coloring of anodized aluminum in cupric sulfate, 24
Visual grading
Grading of softwood lumber using non-destructive techniques, 149

Warm tensile deformation
Flow stress equation of AZ31 magnesium alloy sheet during warm tensile deformation, 29

Water spray
Effect of water spray on friction and wear behaviour of noncommercial and commercial brake pad materials, 135
Wax-coated SiC abrasives
Abrasive jet polishing on SKD61 mold steel using SiC coated with Wax, 318
Wear
Effect of water spray on friction and wear behaviour of noncommercial and commercial brake pad materials, 135
Cutting edge preparation using magnetic polishing and its influence on the performance of high-speed steel drills, 196
Wear action
Investigation of ultrasonic copper wire wedge bonding on Au/Ni plated Cu substrates at ambient temperature, 179
Weld
Experimental and numerical analyses of residual stress distributions in TIG welding process for 304L stainless steel, 383
Welding
On the influence of tool path in friction stir spot welding of aluminum alloys, 309
Wheel topography
Correlation of grinding wheel topography and grinding performance: A study from a viewpoint of three-dimensional surface characterisation, 14
Wire EDM
Influence of secondary electro-conductive phases on the electrical discharge machinability and frictional behavior of ZrO_2-based ceramic composites, 423
Workpiece stiffness
An improved computation model for critical bending force of three-jaw chucks, 124

Ytterbium doped yttrium oxide
Combustion synthesis of Y_2O_3 and Yb–Y_2O_3. Part I. Nanopowders and their characterization, 415
Yttrium oxide
Effect of Y_2O_3 addition on microstructure of Ni-based alloy + Y_2O_3/substrate laser clad, 549

ZrO_2 composite
Influence of secondary electro-conductive phases on the electrical discharge machinability and frictional behavior of ZrO_2-based ceramic composites, 423

ELSEVIER

Volume 208, Issues 1–3, 21 November 2008

Journal of
Materials
Processing
Technology

www.elsevier.com/locate/jmatprotec

Contents

Cellular automaton simulation of grain growth with different orientation angles during solidification process 1
X. Zhan, Y. Wei, Z. Dong

Effects of current frequency on the structural characteristics and corrosion property of ceramic coatings formed on magnesium alloy by PEO technology 9
G.-H. Lv, H. Chen, W.-C. Gu, L. Li, E.-W. Niu, X.-H. Zhang, S.-Z. Yang

Correlation of grinding wheel topography and grinding performance: A study from a viewpoint of three-dimensional surface characterisation 14
A.T. Nguyen, D.L. Butler

Study on the black electrolytic coloring of anodized aluminum in cupric sulfate 24
H.-H. Shih, Y.-C. Huang

Flow stress equation of AZ31 magnesium alloy sheet during warm tensile deformation 29
Y.Q. Cheng, H. Zhang, Z.H. Chen, K.F. Xian

The improvement on capacity retention of silicon/graphite composites with TiN additive as anode materials for Li-ion battery 35
Y.-S. Wu, Y.-H. Lee, Y.-L. Tsai

Numerical analysis of strip edge drop for Sendzimir mill 42
H.-L. Yu, X.-H. Liu, G.-T. Lee, H.-D. Park

Cold rotary forming of thin-wall component from flat-disc blank 53
C.C. Wong, A. Danno, K.K. Tong, M.S. Yong

Microfluidic chip made of COP (cyclo-olefin polymer) and comparion to PMMA (polymethylmethacrylate) microfluidic chip 63
L. Yi, W. Xiaodong, Y. Fan

Rapid reactive synthesis and sintering of textured $Ca_3Co_4O_9$ ceramics by spark plasma sintering 70
Y. Zhang, J. Zhang

The hardenability of austenite with different alloy content and dispersion in dual-phase steels 75
B. Demir, M. Erdoğan

A novel response variable for finite element simulation of hydro-mechanical deep drawing 85
Z. Zhang, S. Zhao, Y. Zhang

A study on gas-assisted injection molding filling simulation based on surface model of a contained circle channel part 90
L. Chen, J. Li, H. Zhou, D. Li, Z. He, Q. Tang

Direct rapid high-temperature alloy prototyping by hybrid plasma-laser technology 99
Y.-P. Qian, J.-H. Huang, H.-O. Zhang, G.-L. Wang

Preparation and mechanical properties of $Fe_3Al(Ti)$/TiC composites 105
J. Li, Q. Liu, R.-x. Shi, Y. Wen, Y.-s. Yin

Fabrication of self-encapsulated nickel microchannels and nickel nanowalls by reactive ion etching 111
P.G. Jung, I.D. Jung, S.M. Lee, J.S. Ko

Plasma electrolytic deposition of titanium dioxide nanorods and nano-particles. 117
T. Paulmier, J.M. Bell, P.M. Fredericks

(Contents continued on page I)

0924-0136(20081121)208:1/3;1-A

(Contents continued from OBC)

An improved computation model for critical bending force of three-jaw chucks 124
P.F. Feng, Z.J. Wu, D.W. Yu, E. Uhlmann

Improvement of shape memory effect in an Fe–Mn–Si–Cr–Ni alloy fabricated by equal channel angular pressing 130
Z. Wei, J. Laizhu, L. Ning, W. Yuhua

Effect of water spray on friction and wear behaviour of noncommercial and commercial brake pad materials 135
N.S.M. El-Tayeb, K.W. Liew

Microwave synthesis of high dielectric constant $CaCu_3Ti_4O_{12}$ 145
H. Yu, H. Liu, D. Luo, M. Cao

Grading of softwood lumber using non-destructive techniques 149
S.-Y. Wang, J.-H. Chen, M.-J. Tsai, C.-J. Lin, T.-H. Yang

The effect of multiphase nitride inclusions on the surface roughness of 2083 plastic molds 159
G. Yingchun, T. Guoyi, W. Junxi, Y. Qiang, M. Mizuno, W. Yongbo

Effect of inverse peritectic reaction on microstructural spheroidization in semi-solid state 165
J.-Y. Li, S. Sugiyama, J. Yanagimoto, Y.-L. Chen, G.-W. Fan

Experimental observation and numerical analysis of cracking phenomena in adjoining Vickers indentations on glass surface 171
B. Zhang, M. Yoshioka, S. Hira

Investigation of ultrasonic copper wire wedge bonding on Au/Ni plated Cu substrates at ambient temperature 179
Y. Tian, C. Wang, I. Lum, M. Mayer, J.P. Jung, Y. Zhou

Characterization and modelling of the residual stresses induced by belt finishing on a AISI52100 hardened steel 187
J. Rech, G. Kermouche, W. Grzesik, C. García-Rosales, A. Khellouki, V. García-Navas

Cutting edge preparation using magnetic polishing and its influence on the performance of high-speed steel drills 196
F.Y. Cheung, Z.F. Zhou, A. Geddam, K.Y. Li

Effect of extrusion on microstructure and properties of a submicron crystalline Cu–5 wt.%Cr alloy 205
W. He, E. Wang, L. Hu, Y. Yu, H. Sun

The prediction of deformation behavior and interfacial friction under hot working conditions using inverse analysis 211
N. Kim, H. Choi

Optimization of injection mold based on fuzzy moldability evaluation 222
J. Cheng, Y. Feng, J. Tan, W. Wei

Study of the correlation between surface generation and cutting vibrations in peripheral milling 229
H. Jiang, X. Long, G. Meng

An experimental study on discharge mediums used for electro-contact discharge dressing of metal-bonded diamond grinding wheel 239
J. Xie, J. Tamaki

Effect of technological parameter on the process performance for electric discharge milling of insulating Al_2O_3 ceramic 245
Y.H. Liu, X.P. Li, R.J. Ji, L.L. Yu, H.F. Zhang, Q.Y. Li

Synthesis of poly(*N*-vinylpyrrolidone)/β-cyclodextrin composite nanofibers using electrospinning techniques 251
J. Bai, Q. Yang, M. Li, C. Zhang, L. Yiaoxian

Structure and luminescent properties of GaN nanorods grown by magnetron sputtering and ammoniating technique 255
J. Chen, C. Xue, H. Zhuang, H. Li, L. Qin, Z. Yang

A tool path generation strategy for three-axis ball-end milling of free-form surfaces 259
T. Chen, Z. Shi

Intensified sintering of iron powders under the action of an electric field: Effect of technologic parameter on sintering densification 264
K. Feng, Y. Yang, M. Hong, J. Wu, S. Lan

Optimal laser-cutting parameters for QFN packages by utilizing artificial neural networks and genetic algorithm 270
M.-J. Tsai, C.-H. Li, C.-C. Chen

Numerical simulation of the densification processing of titanium-matrix coated fiber composites 284
L. Hengjun, Y. Yanqing, H. Bin, Y. Meini, L. Xian

Experimental research on vibration assisted EDM of micro-structures with non-circular cross-section 289
H. Tong, Y. Li, Y. Wang

Durability of concrete made with granite and marble as recycle aggregates..... 299
H. Binici, T. Shah, O. Aksogan, H. Kaplan

On the influence of tool path in friction stir spot welding of aluminum alloys 309
G. Buffa, L. Fratini, M. Piacentini

Abrasive jet polishing on SKD61 mold steel using SiC coated with Wax 318
B.H. Yan, F.C. Tsai, L.W. Sun, R.T. Hsu

Effect of ultrasonic treatment on microstructures of hypereutectic Al–Si alloy 330
H.K. Feng, S.R. Yu, Y.L. Li, L.Y. Gong

Thermal analysis of sponge iron preheating using waste energy of EAF..... 336
E. Hajidavalloo, A. Alagheband

A new method to prepare flame retardant polymer composites..... 342
M. Zhang, P. Ding, B. Qu, A. Guan

Establishment of process model for part strength in stereolithography 348
K. Chockalingam, N. Jawahar, U. Chandrasekar, K.N. Ramanathan

Structure of copper subjected to changes of the loading scheme during rolling 366
W. Bochniak, K. Pantoł

Effect of surface roughness parameters and surface texture on friction and transfer layer formation in tin–steel tribo-system 372
P.L. Menezes, Kishore, S.V. Kailas

Experimental and numerical analyses of residual stress distributions in TIG welding process for 304L stainless steel 383
S.A.A. Akbari Mousavi, R. Miresmaeili

Effect of processing on stress-corrosion behavior of die-cast Mg–Al alloy..... 395
Y. Unigovski, E.M. Gutman, Z. Koren, H. Rosenson, Y. Hao, T. Chen

Ultra-precision turning of electroless-nickel: Effect of phosphorus contents, depth-of-cut and rake angle 400
A. Pramanik, K.S. Neo, M. Rahman, X.P. Li, M. Sawa, Y. Maeda

Evidence of giant magnetoresistance effect in heterogeneous nanogranular films produced by ultrashort pulsed laser deposition..... 409
V. Iannotti, S. Amoruso, G. Ausanio, A.C. Barone, C. Campana, C. Hison, L. Lanotte

Combustion synthesis of Y_2O_3 and Yb–Y_2O_3 Part I. Nanopowders and their characterization 415
R.V. Mangalaraja, J. Mouzon, P. Hedström, I. Kero, K.V.S. Ramam, C.P. Camurri, M. Odén

Influence of secondary electro-conductive phases on the electrical discharge machinability and frictional behavior of ZrO_2-based ceramic composites..... 423
K. Bonny, P. De Baets, J. Vleugels, A. Salehi, O. Van der Biest, B. Lauwers, W. Liu

Flow field characterization of friction stir processing using a particle-grid method 431
B.C. Liechty, B.W. Webb

Net-shape production of graphite parts via powder injection moulding of carbon mesophase 444
B. Derfuss, M. Gruhl, C.A. Rottmair, A. Volek, R.F. Singer

Residual stress during heat treatment of steel grinding balls 450
C. Camurri, C. Carrasco, J. Dille

Gelcasting of metal powders in nontoxic cellulose ethers system 457
Y. Li, Z. Guo, J. Hao, S. Ren

Preparation of fine grain tungsten heavy alloy with high properties by mechanical alloying and yttrium oxide addition..... 463
F. Jing-lian, L. Tao, C. Hui-chao, W. Deng-long

Artificial neural network approach to predict the electrical conductivity and density of Ag–Ni binary alloys 470
M.S. Ozerdem

Analysis of the ageing impact on the strength of the adhesive sealed joints of conveyor belts 477
D. Mazurkiewicz

Electromagnetic impact welding of aluminum to stainless steel sheets 486
S.D. Kore, P.P. Date, S.V. Kulkarni

Synthesis of Ni nanoparticles and their catalytic effect on the decomposition of ammonium perchlorate ... 494
H. Duan, X. Lin, G. Liu, L. Xu, F. Li

Multi-objective optimization of sheet metal forming process using Pareto-based genetic algorithm..... 499
L. Wei, Y. Yuying

Chemical machining of nanocrystalline Ni 507
S. Ho, T. Nakahara, G.D. Hibbard

The effects of surface roughness and nanostructure on the properties of indium tin oxide (ITO) designated for novel optoelectronic devices fabrication 514
G. Kavei, A.M. Gheidari

Studies on chromium/aluminium-doped manganese spinel as cathode materials for lithium-ion batteries—A novel chelated sol–gel synthesis..... 520
R. Thirunakaran, A. Sivashanmugam, S. Gopukumar, C.W. Dunnill, D.H. Gregory

Investigating the machinability evaluation of Hadfield steel in the hard turning with Al_2O_3/TiC mixed ceramic tool based on the response surface methodology 532
J.-T. Horng, N.-M. Liu, K.-T. Chiang

Effect of impact energy on residual stresses induced by hammer peening of 304L plates 542
L. Hacini, N. Van Lê, P. Bocher

Effect of Y_2O_3 addition on microstructure of Ni-based alloy + Y_2O_3/substrate laser clad 549
P. Xu, X. Tang, S. Yao, J. He, G. Xu

Author index..... 556

Subject index 558